Clim. Past Discuss., 5, 1109–1132, 2009
www.clim-past-discuss.net/5/1109/2009/

Climate
of the Past
Discussions

Climate of the Past Discussions is the access reviewed discussion forum of *Climate of the Past*

2-D reconstruction of past sea level (1950–2003) using tide gauge records and spatial patterns from a general ocean circulation model

W. Llovel[1], A. Cazenave[1], P. Rogel[2], A. Lombard[3], and M. Bergé-Nguyen[1]

[1]LEGOS, OMP, 18 avenue Edouard Belin – 31401 Toulouse Cedex 09, France
[2]CERFACS/URA1875, 42, Avenue Gaspard Coriolis, 31057 Toulouse Cedex 01, France
[3]CNES, 18 avenue Edouard Belin – 31401 Toulouse Cedex 09, France

Received: 20 February 2009 – Accepted: 6 March 2009 – Published: 20 March 2009

Correspondence to: W. Llovel (william.llovel@legos.obs-mip.fr)

Published by Copernicus Publications on behalf of the European Geosciences Union.

Abstract

A two-dimensional reconstruction of past sea level is proposed at yearly interval over the period 1950–2003 using tide gauge records at 99 selected sites and 44-year long (1960–2003) 2°×2° gridded dynamic heights from the OPA/NEMO global ocean circulation model with data assimilation. An Empirical Orthogonal Function decomposition of the reconstructed sea level over 1950–2003 displays leading modes that reflect two main components: a long-term (multi-decadal) but regionally variable signal and interannual fluctuations dominated by the signature of El Nino-Southern Oscillation. Tests show that spatial trend patterns of the 54-year long reconstructed sea level (1950–2003) significantly depend on the length of the gridded OPA/NEMO time series used to compute spatial covariance signal used for the reconstruction (i.e., the length of the gridded OPA/NEMO time series). On the other hand, the interannual variability is well reconstructed, even with ∼10-year long of the OPA/NEMO model or satellite altimetry-based sea level grids. The robustness of the results is assessed, leaving out successively each of the 99 tide gauges when reconstructing the sea level signal and then comparing observed and reconstructed time series at the non contributing tide gauge site. The reconstruction performs well at most tide gauges, especially at interannual frequency.

1 Introduction

Sea level is one of the most important climatic indices because it integrates the response of many components of the Earth system to climate change and variability: ocean and its interaction with the atmosphere, land ice and terrestrial waters. Even solid Earth processes have some impact on sea level. Since the beginning of the 1990s, sea level is precisely measured by satellite altimetry systems (i.e., Topex/Poseidon, Jason-1 and now Jason-2) with global coverage. The satellite observations have revealed that sea level does not rise uniformly: some regions rise faster than the global mean, other regions display sea level fall (Bindoff et al., 2007). It has been further shown that the main cause of regional variability in the rates of sea level change is non uniform thermal expansion of the oceans (Cabanes et al., 2001; Cazenave and Nerem, 2004). Studies have also established that during the past few decades, trend patterns in thermal expansion were not stationary but fluctuated both in space and time in response to ENSO (El Nino-Southern Oscillation), NAO (North Atlantic Oscillation) and PDO (Pacific Decadal Oscillation) (Lombard et al., 2005). This suggests that present-day sea level trend patterns may be representative neither of past nor future. Yet, it is important to know past regional variability, for example to validate climate models used to predict future sea level change at regional and global scales. Important uncertainties in climate projections affect regional changes and decadal fluctuations in future sea level (Meehl et al., 2007).

Unfortunately, for the last century, information about sea level is sparse and essentially based on tide gauge records along islands and continental coastlines. Such a data set cannot inform upon open ocean regional variability. For that reason, several previous studies have attempted to reconstruct past decades sea level in two dimensions (2-D), combining sparse but long tide gauge records with global gridded (i.e., 2-D) sea level (or sea level proxies) time series of limited temporal coverage (Chambers et al., 2002; Church et al., 2004; Berge-Nguyen et al., 2008). The present study has a similar objective: it expands an earlier work by Bergé-Nguyen et al. (2008) (hereafter denoted as BN08) but makes use of improved information for the 2-D fields used for the reconstruction. Previous studies used global sea level grids based on Topex/Poseidon satellite altimetry of limited (<15 years) temporal coverage (e.g., Chambers et al., 2002; Church et al., 2004) or decade-long gridded time series of thermal expansion based on in situ hydrographic data available that suffer sparse geographic coverage in the southern hemisphere and at ocean depths below ~700 m (e.g., BN08). In this study, we use global dynamic heights grids from an Ocean General Circulation Model (OGCM; the OPA/NEMO model constrained by data assimilation; Madec et al., 1998) available over a 46-year time span (1960–2005), in combination with tide gauge records (that cover the period 1950–2003). Here we only consider a 44-year (1960–2003) time span for the OPA/NEMO outputs to be in line with the tide gauge records length. The advantage of using such a long data set is twofold: (1) the 44-year long coverage better samples the probable non stationarity of altimetry-based spatial patterns (see BN08 for a discussion), (2) the assimilation, optimizing the information brought by the observations and the dynamics, partially solves the problem of poor geographical and deep ocean coverage of in situ hydrographic data. We present below the resulting sea level reconstruction over the 1950–2003 time span.

2 Method

Several studies have developed methods for reconstructing past 2-D time series of oceanographic (e.g., sea surface temperature, sea surface height) or atmospheric (e.g., surface wind speed, surface pressure) fields by combining 2-D grids of limited temporal length (in general available from remote sensing observations over the last 2 decades or less) with historical (several decade-long), sparse 1-D records (e.g., Smith et al., 1994, 1996; Kaplan et al., 1998; Church et al., 2004, 2006; Chambers et al., 2002; Alvera-Azcarate et al., 2004; Rayner et al., 2003). The general approach uses Empirical Orthogonal Empirical Functions (EOF) decomposition (e.g., Preisendorfer, 1988; Toumazou and Cretaux, 2001) of the 2-D time series to extract the dominant modes of spatial variability of the signal. These EOF spatial modes are then fitted to the 1-D records to provide reconstructed multidecade-long 2-D fields. Different computational variants of the method have been developed to estimate the reconstructed long-term 2-D fields depending on the use of a priori information and data errors (e.g. Kaplan et al., 1998; Rayner et al., 2003; Church et al., 2004) or not (Smith et al., 1996). Alternative methodology based on a cross-validation technique has also been developed, mainly for reconstruction of incomplete data sets (e.g., Alvera-Azcarate et al., 2004). When applied to long-term past reconstruction, an implicit assumption of the method is the temporal stationarity of the spatial patterns recovered from the EOF modes of the short-term 2-D fields. The spatial covariance obtained from the 2-D fields must indeed be able to describe the spatial covariance over the entire period of the reconstruction (e.g., Smith et al., 1996). If the dominant modes of spatial variability have characteristic time scales longer than the time interval covered by the 2-D fields, EOF spatial modes may incompletely capture the relevant long-term signal. In particular the multidecadal component of the reconstructed signal may be in error.

We briefly summarize below the methodology. Let us call Fo(x,y,t) and Go(x,y,t) observed global gridded short-term fields and sparse, incomplete long-term sea level data respectively, with x,y and t being cartesian coordinates and time. The time span T_f covered by the Fo(x,y,t) fields is basically shorter than that – called Tg – of the reconstructed fields. Here, Fo(x,y,t) correspond to gridded dynamic ocean heights from the OPA/NEMO models over 1960–2003, while the Go(x,y,t) – spatially incomplete – fields correspond to tide gauge records over 1950–2003. The Fo(x,y,t) function is expressed as a sum of combined $X_n(x,y)$ spatial modes and $e_n(t)$ principal components using an EOF decomposition. The objective of the reconstruction is to compute 2-D Go(x,y,t) fields with global spatial coverage – hereafter denoted as $G_R(x,y,t)$ – over the Tg time span (here 1950–2003). The 2-D reconstructed sea level fields are written as $G_R(x,y,t)=\sum[X_n(x,y)\ Y_n(t)]$ where $Y_n(t)$ are new principal components computed at each time step t and mode n, through a least-squares fit that minimizes the quantity ε expressed by $\varepsilon=[\mathrm{Go}(x,y,t)-\sum[X_n(x,y)Y_n(t)]]^2$. For more details, see BN08.

3 Tide gauge data

The tide gauge data used in this study are extracted from the Permanent Service for Mean Sea Level (PSMSL) database (Woodworth and Player, 2003). We use Revised Local Reference (RLR) tide gauge records (annual averages). Detailed descriptions of these time series are available at www.pol.ac.uk/psmsl. From the whole set of records available, we consider stations that have almost complete temporal coverage over 1950–2003. A very careful selection of sites has been realized. Compared to the

118 sites considered in BN08, here we use only 99 sites, deleting a number of tide gauge records with suspect behaviors (e.g., offsets). Search of information on internet about the deleted sites indicates that in almost all cases, tectonic (e.g., co seismic offset or post seismic relaxation of the crust), volcanic or ground subsidence of anthropogenic origin, could be identified as causes of the spurious bias or trends. The tide gauge records are corrected for post-glacial isostatic adjustment (GIA) using the ICE-5G model (Peltier, 2001). We also correct the tide gauge time series for the inverted barometer response of sea level to atmospheric loading using surface pressure fields from the National Centers for Environmental Project (NCEP) (Kalnay et al., 1996). One problem with tide gauge records is that measurements are made in a local datum that varies from one site to another. By working with the derivatives, this problem can be overcome (e.g., Holgate and Woodworth, 2004; Holgate, 2007). Nevertheless, this approach cannot be used here. Hence, we choose another approach (e.g., Kuo et al., 2007) consisting of subtracting to each sea level record a mean value computed over the 1950–2003 time span (note that the 99 tide gauge records are almost complete; when small gaps (<3 years) are observed, we linearly interpolate missing data). Figure 1 shows the distribution of the tide gauge sites used in this study (superimposed on a map of OPA/NEMO dynamic height spatial trends).

4 OPA/NEMO ocean general circulation model outputs

The ocean reanalyse used in this study has been produced with a 3-dimensional variational assimilation system (Daget and Weaver, 2009; Ingleby and Huddleston, 2007) applied to the OPA/NEMO ocean circulation model (Madec et al., 1998). The model resolution, 2° on average, with a latitudinal refinement in the tropics, is coarse but appropriate for the multidecadal period of interest here. The model is forced by the standard reanalyse ERA40 heat fluxes (Uppala et al., 2005) and corrected water fluxes (Troccoli and Kalberg, 2004). From September 2002 onwards, when ERA40 terminates, ECMWF (European Center for Meteorological Forecast) operational surface fluxes were used as forcing. Quality controlled temperature and salinity profiles from the EN3 oceanographic data base (Ingelby and Huddleston, 2007) are assimilated every 10 days from January 1960 to December 2006. But the model outputs are on a monthly basis. Annual means are used to compute EOFs.

As described in Roullet and Madec (2000), the model is formulated with a prognostic free surface, constant volume and salt preserving scheme, assuming that the mean sea level does not vary. Hence, both forcing and data assimilation have been designed to ensure that no drift in the mean sea level occurs. In particular, water flux balance between precipitation, evaporation and runoff is set to zero in the free surface equation, and assimilation increments (i.e. the model corrections applied every 10 days to the model using temperature and salinity observations) are built under the constraint that the sea level increment is zero on spatial average (Weaver et al., 2005). In addition, the model is relaxed towards a climatology (Levitus et al., 1994) poleward of 60° and in the semi-enclosed seas, so that interannual variations in those regions are almost suppressed. On the other hand, no constraint is applied over open ocean areas.

In Fig. 1 are displayed sea level trends from the OPA/NEMO model with data assimilation over 1960–2003. For the reasons explained above, the map has zero global mean (uniform) trend. Important regional variability is observed, especially in the western parts of the basins. The strongest spatial patterns are located close to the western boundary currents (e.g. Gulf Stream in the Northwestern Atlantic, Kuroshio in the Northwestern Pacific; Malvinas Current in the Southwestern Atlantic).

5 Sea level reconstruction

5.1 Reconstructed spatial trend patterns over 1950–2003

We reconstructed 2-D sea level grids at yearly interval over 1950–2003 combining spatial EOFs of the OPA/NEMO grids over 1960–2003 (44 years of gridded data) with 99 tide gauge time series covering the 1950–2003 time span. Most of the variance of the reconstructed sea level is included in the first 10–20 modes. Higher-order modes exhibit essentially noise. In the following, we consider as nominal case (called case 1), the first 10 modes when reconstructing sea level (with 75% of the total signal variance). Corresponding reconstructed spatial trend map over 1950–2003 is presented in Fig. 2a. We note that trend amplitudes are everywhere higher than in the model trend map (Fig. 1) but extrema are located at the same places (e.g., Gulf Stream, Kuroshio; Malvinas Current, etc.). For comparison we also show the spatial trend map with the first 20 modes used for the reconstruction (Fig. 2b). The 20 modes case contains more energy but is also noiser (as discussed in BN08).

In order to assess the benefit of using multi-decadal gridded OPA/NEMO time series for reconstructing past sea level, we performed tests with shorter model time series. Four cases are considered: 31 years of OPA/NEMO grids (1973–2003) – case 2 –, 21 years of OPA/NEMO grids (1983–2003) – case 3 –, and 11years of OPA/NEMO grids (1993–2003) – case 4. Case 4 can be compared with studies that use decade-long Topex/Poseidon altimetry grids for sea level reconstruction (e.g., Chambers et al., 2002; Church et al., 2004). Corresponding reconstructed spatial trend maps are presented in Fig. 3a, b, c (using for each case, the number of modes that correspond to 75% of the total variance). Significant regional differences are noticed between for the first two cases (44 years and 31 years of OPA/NEMO grids respectively) and cases 3 and 4 (21 years and 11 years of OPA/NEMO grids respectively), in particular in the North Atlantic, Indian Ocean, Austral Ocean and Northeast Pacific. On the other hand, spatial trend patterns for cases 1 and 2 give are quite in agreement. A similar observation can be done for cases 3 and 4. We thus observe a transition in reconstructed trends when OPA/NEMO grids length increases from ~20 years to ~30 years. As discussed below, the low-frequency sea level signal may not be well captured in cases that use short spatial grids for the reconstruction (cases 3 to 5). In the latter cases, patterns representing interannual variability dominate the reconstructed spatial trends.

To compare with case 4, we also show in Fig. 3d reconstructed sea level trends (over

1950–2003) using 11 years (1993–2003) of Topex/Poseidon sea level grids (case 5). The latter case is very similar to Church et al. (2004)'s study. Although case 5 contains shorter wavelength signal than case 4, spatial trend patterns show similar large scale features.

We performed EOF decompositions of the reconstructed sea level grids over 1950–2003 for cases 1 to 4. Figure 4a, b, c, d show the two leading EOF modes for each case. Mode 1 temporal curve (principal component) of nominal case is dominated by a positive slope. Associated mode 1 spatial map closely resembles case 1 reconstructed trend map (Fig. 2a), with strong signal in the Austral Ocean (especially Southeast of Africa). This suggests that the reconstructed trend map for the nominal case mostly reflects a long-term (multi-decadal), regionally variable signal. Mode 2 of case 1 (Fig. 4a right panel) is dominated by the interannual variability and displays clear signature of ENSO in the tropical Pacific: the Southern Oscillation Index (SOI) – a proxy of ENSO – is significantly correlated (61%) to the temporal curve on which is it superimposed. It is worth mentioning that the spatial map of mode 2 (case 1) is very similar to the satellite altimetry-based sea level trend map over 1993–2003 (see below). Hence, whilst mode 1 reflects long-term, multidecadal signal, mode 2 mostly reflects ENSO-type interannual variability.

The two leading modes of case 2 (Fig. 4b) closely resemble those of case 1. The first EOF mode of cases 3 and 4 reflects interannual variability (as mode 2 of cases 1 and 2). This is illustrated in Fig. 5 which shows energy spectra of the interannual signal for cases 1, 4 and 5 (i.e., spectra of the temporal curves of corresponding EOF modes). SOI spectrum is superimposed. The agreement between the four curves is striking. Peaks in the 3–5 yr and 10–15 yr wavebands dominate. They mainly reflect ENSO frequency and associated decadal modulation. On the other hand, looking at the long-term signal (e.g., comparing modes 1 of case 1 and 2 with mode 2 of cases 3 and 4), we note significant difference in the spatial maps, suggesting that multidecadal fluctuations are only partly recovered when using short gridded time series for the reconstruction (e.g., cases 3 and 4).

5.2 Robustness of the reconstruction

5.2.1 Sea level reconstruction over the altimetry (1993–2003) period using the OPA/NEMO EOFs

A way to check the validity of the reconstruction is to look at the reconstructed sea level trends over the altimetry period (here 1993–2003) for which we trust the spatial trend patterns. Figure 6a shows the reconstructed spatial trend map over 1993–2003 based on 44-years of OPA/NEMO grids. We note that it closely agrees with observed satellite altimetry trend map over 1993–2003 (Fig. 6b, uniform trend removed), although the latter contains more short-wavelength signal (the OPA/NEMO model has a 2° resolution, thus does not contain as much short wavelength signal as sea level based on multisatellite altimetry). However we note that large-scale patterns are very similar to the observed ones. As noticed above, there is striking similarity between 1993–2003 reconstructed sea level trends and spatial patterns of nominal case's mode 2.

5.2.2 Cross-validation of reconstructed series and tide gauge records

Another way to check the robustness of the reconstruction consists of reconstructing sea level leaving out successively each one of the 99 tide gauge records (thus each of these 99 reconstructions now uses a set of 98 tide gauges, with different distribution from one case to another). For each deleted tide gauge, we compare the reconstructed sea level time series at the tide gauge site with the PSMSL data (reconstructed sea level is averaged within 2° around the tide gauge site). For this test we consider two cases: case1 (reconstruction with 44 years of gridded OPA/NEMO grids) and case 5 (reconstruction with 11 years of Topex/Poseidon gridded data). Figure 7a shows a subset of 9 comparisons (corresponding site locations are enhanced by stars in Fig. 1). Figure 7b is similar to Fig. 7a except for the trend which has been removed. We note that in general interannual to decadal variability is well reproduced (Fig. 7b). The average correlation between (detrended) reconstructed and observed sea level at the

99 sites amounts to ~60%. The trends also agree well in most cases, although not everywhere. Sites where trends disagree concern mostly northeast Atlantic areas (e.g., North Shields, Lowestoft, Santander, La Coruna, and Vigo). We suspect that this is due to local underestimated variability in the OPA/NEMO reanalysis, especially in the first 20 years of the period. Similar comparison with case 5 (not shown) shows very similar results for the detrended time series. To see the above results in another way, we have computed the root mean squared (i.e. rms) differences between (detrended) reconstructed and observed sea level time series as well as rms trend differences. Corresponding histograms for the two cases (case 1 and case 5) are shown in Fig. 8. Rms (detrended) sea level differences are included in the 15–60 mm but histogram for case 1 is more spread than for case 5. Figure 9 shows plots of reconstructed sea level trends at the 99 tide gauges as a function of observed trends for the two cases (case 1 and case 5). Here, we see that case 1 gives better results than case 5, with higher correlation. These comparisons indicate that the reconstruction performs well at the interannual time scale (as previously found by Chambers et al., 2002 and Church et al., 2004), with better results for case 5 than case 1. On the other hand, case 1 gives much better results for the trends (hence at multidecadal time scale) than case 5.

6 Conclusions

We have performed a new 2-D sea level reconstruction over 1950–2003. The main change compared to previous published results (e.g., Chambers et al., 2002; Church et al., 2004; Berge-Nguyen et al., 2008) is the use of 44-year long gridded sea level data set from the OPA/NEMO ocean circulation model with assimilation. This allows us to compute spatial EOFs over a >40 yr time span, long enough to capture the multidecadal variability in regional sea level (in addition to the interannual variability). Hopefully, this may prevent from problems due to the use of short-term altimetry grids. Another advantage is the good spatial sampling of the OPA/NEMO outputs compared to in situ-based thermal expansion data (as in BN08). The main conclusion of this study is that using spatial EOFs computed over a short time span (e.g., ∼10–20 years) leads to 2-D reconstructed trend patterns significantly different than when >40 years of EOFs are used. The latter case, not only captures the interannual variability (related to ENSO and possibly NAO and PDO) but also the multidecadal variability. Even if they have local deficiencies, such 2-D reconstructed sea level time series based on low resolution ocean reanalyze are able to bring physically consistent large-scale, low-frequency patterns associated with major climate modes of variability.

As a final remark, we think that the use of OGCM outputs is a step towards better reconstruction of long-term sea level time series (at least waiting for global multidecadal altimetry records). Future improvement is expected by using new generation of eddy-permitting OGCM outputs with higher spatial resolution (e.g., 0.25°×0.25°) in which some local misbehaviors can be corrected. This would provide finer description of the spatial trend patterns. Progress in this direction is already underway.

Acknowledgements. Nicolas Daget and A. T. Weaver are thanked for their provision of the ocean reanalysis data. These data were produced for the EU FP6 Integrated Project ENSEMBLES (Contract number 505539), whose support is gratefully acknowledged. William Llovel PhD grant is supported by CNRS and Region Midi-Pyrenees..

The publication of this article is financed by CNRS-INSU.

References

Alvera-Azcarate, A., Barth, A., Rixen, M., and Beckers, J. M.: Reconstruction of incomplete oceanographic data sets using empirical orthogonal functions: applications to the Adriatic sea surface temperature, Ocean Model, doi:10.1016/j.ocemod.2004.08.001, 2004.

Berge-Nguyen, M., Cazenave, A., Lombard, A., Llovel, W., Viarre, J., and Cretaux, J. F.: Reconstruction of past decades sea level using thermosteric sea level, tide gauge, satellite altimetry and ocean reanalysis data, Global. Planet. Change, 62, 1–13, 2008.

Bindoff, N., Willebrand, J., Artale, V. , Cazenave, A., Gregory, J. , Gulev, S., Hanawa, K., Le Quéré, C., Levitus, S., Nojiri, Y., Shum, C. K., Talley, L., and Unnikrishnan, A.: Observations: oceanic climate and sea level, in: Climate change 2007: The physical Science Basis. Contribution of Working Group I to the Fourth Assessment report of the Intergouvernmental Panel on Climate Change, edited by: Solomon, S., Qin, D., Manning, M., Chen, Z., Marquis, M., Averyt, K. B., Tignor, M., and Miller, H. L., Cambridge University Press, Cambridge, UK, and New York, USA., 385–428, 2007.

Cabanes, C., Cazenave, A., and Le Provost, C.: Sea level rise during past 40 years determined from satellite and in situ observations, Science, 294, 840–842, 2001.

Cazenave A. and Nerem, R. S.: Present-day sea level change: observations and causes, Rev. Geophys., 42, RG3001, doi:8755-1209/04/2003RG000139, 2004.

Chambers, D. P., Mehlha, C. A., Urban, T. J., and Nerem, R. S.: Analysis of interannual and low-frequency variability in global mean sea level from altimetry and tide gauges, Phys. Chem. Earth, 27, 1407–1411, 2002.

Church, J. A., White, N. J., Coleman, R., Lambeck, K., and Mitrovica, J. X.: Estimates of the regional distribution of sea-level rise over the 1950 to 2000 period, J. Climate, 17(13), 2609–2625, 2004.

Church, J. A., White, N. J., and Hunter, J. R.: Sea-level rise at tropical Pacific and Indian Ocean islands, Global Planet. Change, 53(3), 155–168, 2006.

Daget, N. and Waever, A. T.: A three-dimensional ensemble variational data assimilation system for the global ocean: Sensitivity to the observation- and background-error variance formulation, Q. J. Roy. Meteor. Soc., in press, 2009.

Holgate, S. J. and Woodworth, P. L.: Evidence for enhenced coastal sea level rise during the 1990s, Geophys. Res. Lett., 31, L07305, doi:10.1029/2004GL019626, 2004.

Holgate, S. J.: On the decadal rates of sea level change during the twentieth century, Geophys. Res. Lett., 31, L01602, doi:10.1029/2006GL028492, 2007.

Ingleby, B. and Huddleston, M.: Quality control of ocean temperature and salinity profiles – historical and real-time data, J. Mar. Sys., 65, 148–175, 2007.

Kalnay, E., Kanamitsu, M., Kistler, R., Collins, W., Deaven, D., Gandin, L., Iredell, M., Saha, S., White, G., Woollen, J., Zhu, Y., Leetmaa, A., Reynolds, B., Chelliah, M., Ebisuzaki, W., Higgins, W., Janowiak, J., Mo, K. C., Ropelewski, C., Wang, J., Roy, J., and Joseph, D.: The NCEP/NCAR 40-year reanalysis project,. B. A. Meteor. Soc., 77, 437–471, 1996.

Kaplan, A., Cane, M. A., Kushnir, Y., Clement, A. C., Blumenthal, M. B., and Rajagopalan, B.: Analyses of global sea surface temperature 1856–1991, J. Geophys. Res., 103, 18567–18589, 1998.

Kuo, C., Shum, C. K., Braun, A., Cheng, K., and Yi, Y.: Vertical motion determined using satellite altimetry and tide gauges, satellite altimetry over land and coastal zones: challenges and applications, special issue Terrestrial, Atmospheric and Oceanic sciences (TAO), 2007.

Levitus, S., Burgett, R., and Boyer, T. P.: World Ocean Atlas (National Oceanic and Atmospheric Administration, Silver Spring, MD), 3–4, 1994.

Lombard, A., Cazenave, A., Le Traon, P. Y., and Ishii, M.: Contribution of thermal expansion to present-day sea level rise revisited, Glob. Plan. Change, 47, 1–16, 2005.

Madec, G., Delecluse, P., Imbard, M., and Levy, C.: OPA 8.1 Ocean General Circulation Model reference manual. Notes du pôle de modélisation, Institut Pierre Simon Laplace (IPSL), France, 1998.

Meehl, G. A., Stocker, T. F., Collins, W. D., Friedlingstein, P., Gaye, A. T., Gregory, J. M., Kitoh, A., Knutti, R., Murphy, J. M., Noda, A., Raper, S. C. B., Watterson, I. G., Weaver, A. J., and Zhao, Z.-C.: Global Climate Projections, in: Climate Change 2007: The Physical Science Basis. Contribution of Working Group I to the Fourth Assessment Report of the Intergovernmental Panel on Climate Change, edited by: Solomon, S., Qin, D., Manning, M., Chen, Z., Marquis, M., Averyt, K. B., Tignor, M., and Miller, H. L., Cambridge University Press, Cambridge, United Kingdom and New York, NY, USA, 2007.

Peltier, W. R.: Global glacial isostatic adjustment and modern instrumentatal records of relative sea level history, in: Sea Level Rise, History and Consequences, edited by: Douglas, B. C., Kearney, M. S., and Leatherman, S. P., Academic Press, San Diego, 65–95, 2001.

Preisendorfer, R. W.: Principal component Analysis in Meteorology and Oceanography. Developments in Atmospheric Science, 17. Elsevier, 425 pp., 1988.

Rayner, N. A., Parker, D. E., Horton, E. B., Foll, C. K., Alexer, L. V., Powell, D. P., Kent, E. C., and Kaplan, A.: Global analyses of SST, sea ice, and night marine air temperature since the late nineteenth century, J. Geophys. Res., 108, 4407, doi:10.1029/2002JD002670, 2003.

Roullet, G. and Madec, G.: Salt conservation, free surface and varying volume: a new formulation for Ocean GCMs, J. Geophys. Res., 105, 23927–23942, 2000.

Smith, T. M., Reynolds, R. W., and Ropelewski, C. F.: Optimal averaging of seasonal sea surface temperatures and associated confidence intervals (1860–1989), J. Clim., 7, 949–964, 1994.

Smith, T. M., Reynolds, R. W., Livezey, R. E., and Stockes, D.: Reconstruction of historical sea surface temperature using Empirical Orthogonal Functions, J. Climate, 9, 1403–1420, 1996.

Toumazou, V. and Cretaux, J. F.: Using a Lanczos eigensolver in the computation of Empirical Orthogonal Functions, Mon. Weather Rev., 129, 1243–1250, 2001.

Troccoli, A. and Kallberg, P.: Precipitation correction in the ERA-40 reanalysis, ERA-40 Project Report Series 13, ECMWF, 2004.

Uppala, S. M., da Costa Bechtold, V., Fiorino, M., Gibson, J. K., Haseler, J., Hernandez, A., Kelly, G. A., Li, X., Onogi, K., Saarinen, S., Sokka, N., Allan, R. P., Andersson, E., Arpe, K., Balmaseda, M. A., Beljaars, A. C. M., van de Berg, L., Bidlot, J., Bormann, N., Caires, S., Chevallier, F., Dethof, A., Dragosavac, M., Fisher, L., Fuentes, M., Hagemann, S., Hólm, E., Hoskins, B. J., Isaksen, L., Janssen, P. A. E. M., Jenne, R., McNally, A. P., Mahfouf, J.-F., Morcrette, J. J., Rayner, N. A., Saunders, R. W., Simon, P., Sterl, A., Trenberth, K. E., Untch, A., Vasiljevic, D., Viterbo, P., and Woollen, J.: The ERA-40 re-analysis, Q. J. Roy. Meteor. Soc., 131, 2961–30128, 2005.

Weaver, A. T., Deltel, C., Machu, E., Ricci, S., and Daget, N.: A multivariate balance operator for variational ocean data assimilation, Q. J. Roy. Meteor. Soc., 131, 3605–3625, 2005.

Woodworth, P. L. and Player, R.: The permanent service for mean sea level: an update to the 21st century, J. Coastal. Res., 19, 287–295, 2003.

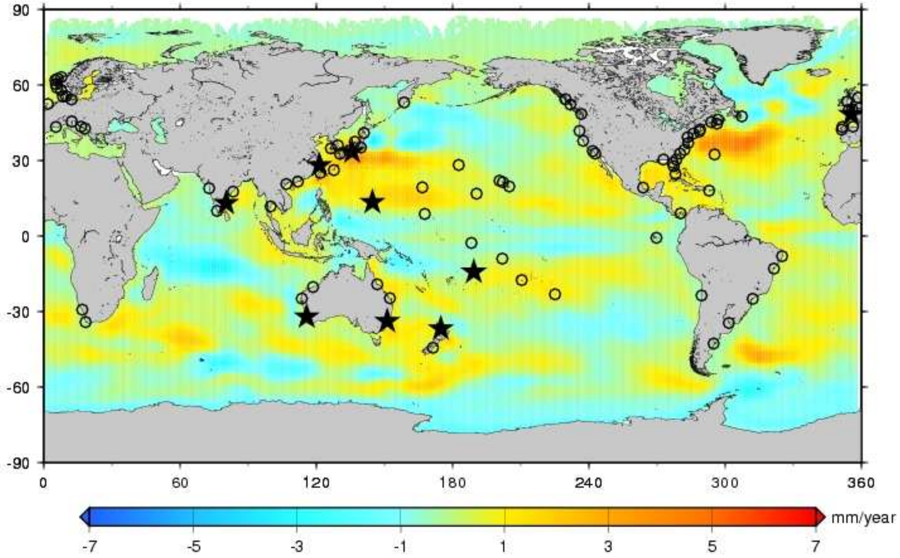

Fig. 1. Location map of the 99 tide gauges (open circles) used in this study. Stars correspond to the comparison sites with records shown in Fig. 7. The background map shows the OPA/NEMO spatial sea level trends computed over 1960–2003 (in mm/yr).

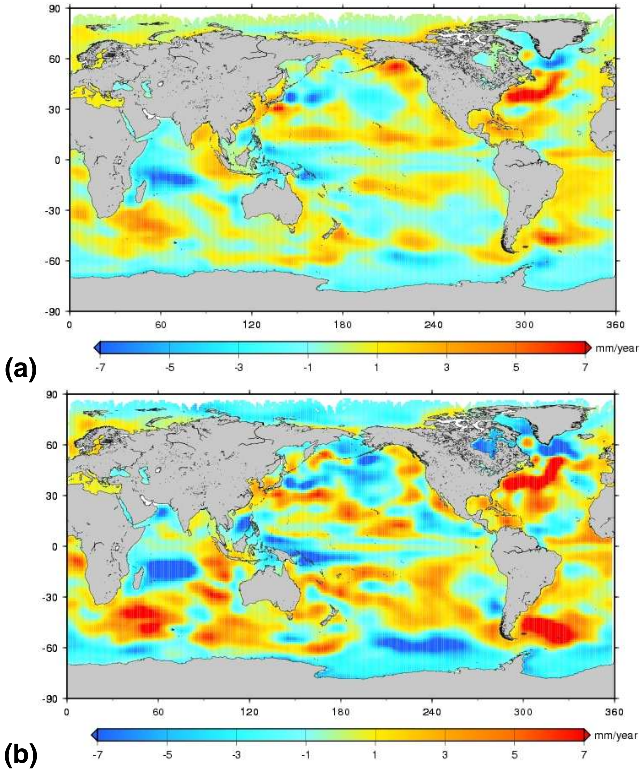

Fig. 2. **(a)** Spatial trend map over 1950–2003 of reconstructed sea level (with 10 modes for the reconstruction); nominal case (case 1). **(b)** Same as (a) but with 20 modes for the reconstruction. Unit: mm/yr.

Title Page
Abstract
Introduction
Conclusions
References
Tables
Figures
◀I
▶I
◀
▶
Back
Close
Full Screen / Esc
Printer-friendly Version
Interactive Discussion

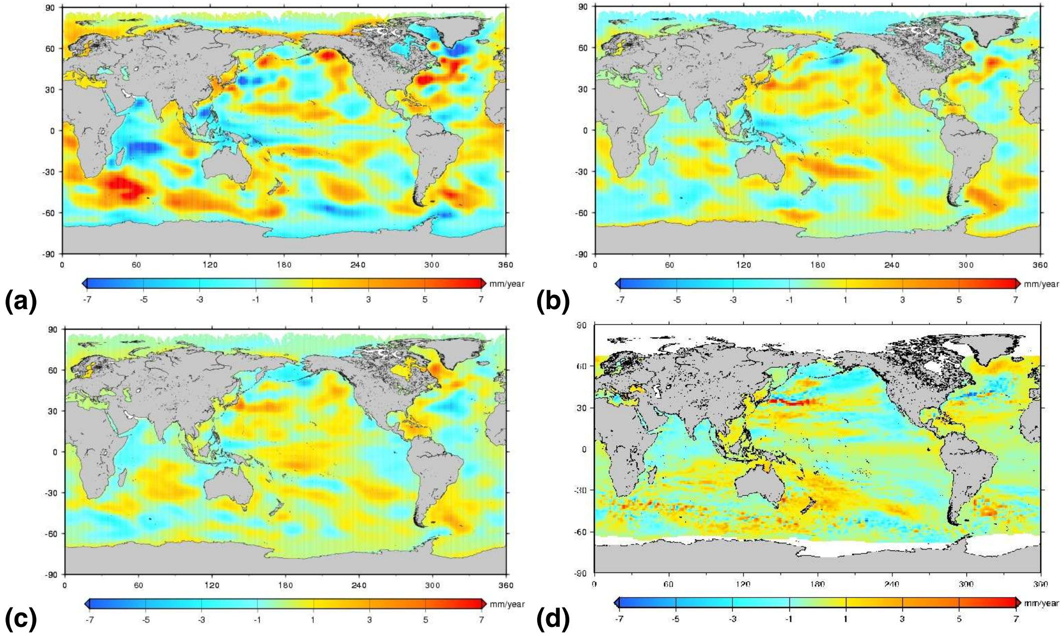

Fig. 3. Spatial trend map over 1950–2003 of reconstructed sea level. **(a)** spatial EOFs from OPA/NEMO over 1973–2003 (case 2); **(b)** spatial EOFs from OPA/NEMO over 1983–2003 (case 3); **(c)** spatial EOFs from OPA/NEMO over 1993–2003 (case 4); **(d)** spatial EOFs from Topex/Poseidon altimetry (case 5). Unit: mm/yr.

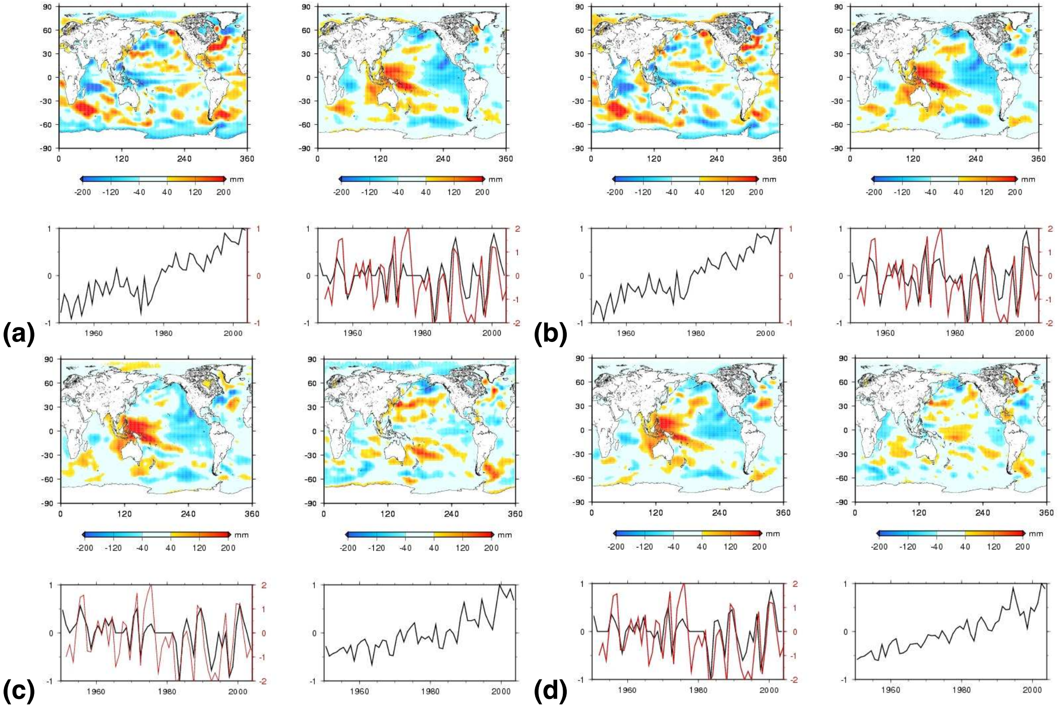

Fig. 4. **(a)** EOF decomposition over 1950–2003 for nominal case (case 1): left: mode 1; right mode 2 (SOI index is superimposed on the temporal curve). **(b)** same as (a) but for case 2; **(c)** same as (a) but for case 3; **(d)** same as (a) but for case 4.

Title Page
Abstract
Introduction
Conclusions
References
Tables
Figures
◀◀
▶▶
◀
▶
Back
Close
Full Screen / Esc
Printer-friendly Version
Interactive Discussion

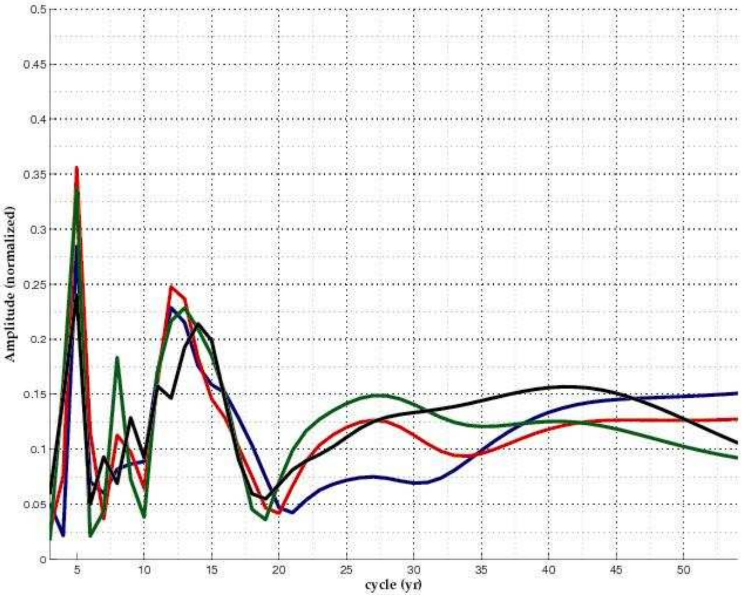

Fig. 5. Energy spectrum of the interannual variability for cases 1 (blue curve), 4 (red curve) and 5 (green curve) and SOI index (black curve).

Title Page
Abstract | Introduction
Conclusions | References
Tables | Figures
I◀ | ▶I
◀ | ▶
Back | Close
Full Screen / Esc
Printer-friendly Version
Interactive Discussion

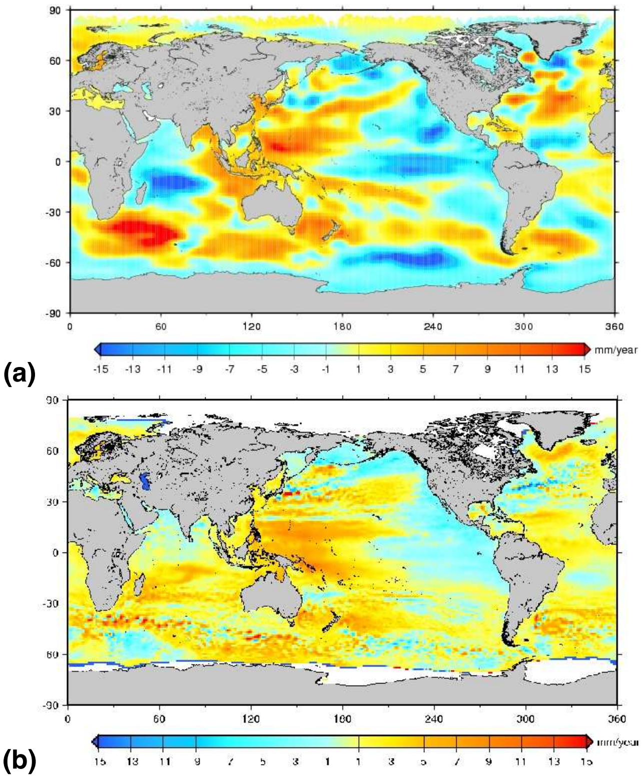

Fig. 6. Spatial sea level trend map over 1993–2003. **(a)** reconstructed sea level for nominal case. **(b)** observed sea level trends from satellite altimetry (uniform trend removed). Unit: mm/yr.

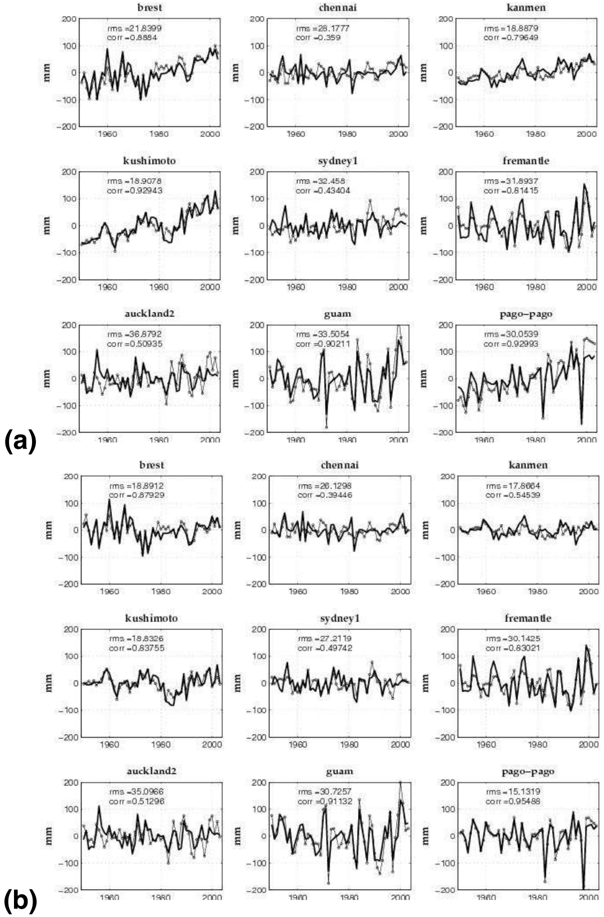

Fig. 7. (a) Subset of 9 tide gauges not used in the reconstruction; observed record (solid curve); reconstructed sea level curve (thin dotted curve). **(b)** same as (a) but with mean trend removed.

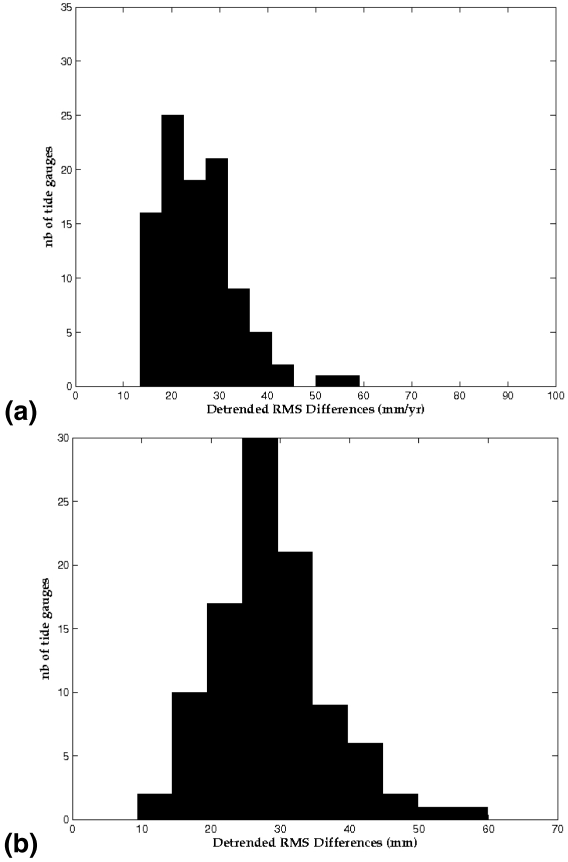

Fig. 8. **(a)** histogram of detrended sea level rms differences (reconstructed – case 1 – minus observed); **(b)** same as (a) but for case 5. Unit: mm/yr.

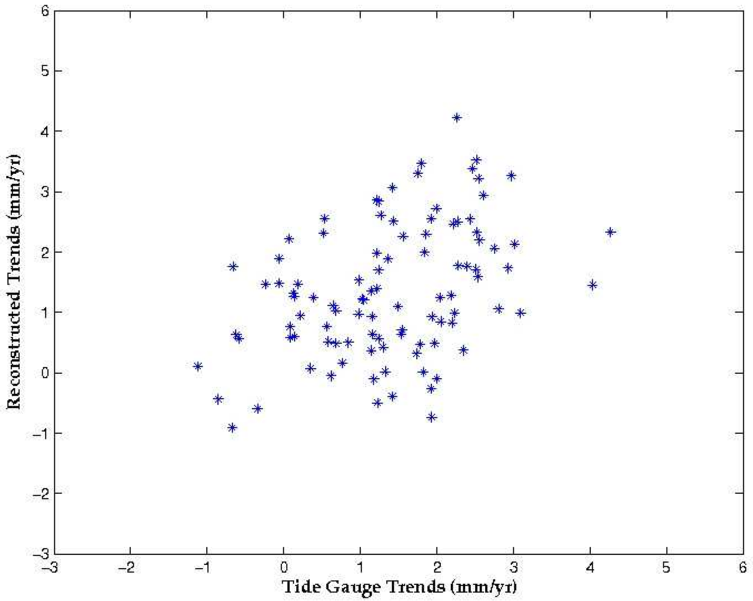

Fig. 9. Plot of the reconstructed trends versus observed trends at the 99 tide gauge sites. **(a)** case 1; **(b)** case 5.